Smartphone-based WiFi FTM Fingerprinting Approach with Map-aided Particle Filter

Meng Sun[1,2], Yunjia Wang[1], Keqiang Liu[3],
Cedric De Cock[2], Wout Joseph[2], *Senior Member, IEEE*, David Plets[2], *Member, IEEE*
[1] School of Environment and Spatial Informatics, China University of Mining and Technology, Xuzhou, China
[2] INTEC-WAVES, Ghent University-IMEC, Ghent, Belgium
[3] Zhejiang Deqing Zhilu Navigation Technology Co., Ltd, Huzhou, China
E-mail: msun@cumt.edu.cn

***Abstract*—Smartphone-based WiFi ranging positioning based on fine time measurement (FTM) always collapses in real-life scenarios. In this work, a novel map-aided particle filter (PF)-based WiFi FTM fingerprinting approach is proposed to address the poor performance of the WiFi FTM ranging positioning. Different from manually collecting fingerprints, this approach utilizes the theoretical received signal strength and geometric distances between the access points and reference points as the fingerprints, which means less labour-intensive work. For accurate WiFi position estimation, a map-aided PF is designed to find the optimal position. Extensive experiments are carried out in the non-line-of-sight (NLoS) and mixed line-of-sight/non-line-of-sight (LoS/NLoS) environments, and the testing results show that the accuracy and stability of FTM fingerprinting are improved by using the mixed RSS and ranging data fingerprints. The minimal mean location errors (MEs) of the PF-based WiFi FTM fingerprinting in NLoS and mixed LoS/NLoS conditions are 1.70 m and 1.85 m, respectively. Compared to the classic weighted least square method, the MEs are reduced by 54.91% and 45.43%, respectively. The testing results demonstrate that the PF-based FTM fingerprinting is an effective approach that provides satisfactory localization results in real-life indoor environments.**

***Index Terms*—Indoor Localization, WiFi FTM, WiFi ranging, Fingerprinting, RSS, RTT, Particle filter, Map, LoS, NLoS**

I. Introduction

As a key technology for smart cities, indoor positioning has always been a popular research topic for the community. Tracking the positions of the objects indoors builds on wireless signals from WiFi [1], Bluetooth [2], UWB [3], RFID [4], etc., or on image-based approaches including visual positioning [5], simultaneously localization and mapping [6], or the infrastructure-free methods using magnetic field [7], pedestrian dead reckoning (PDR) [8], or (un)modulated visible light positioning ((u)VLP) [9]. The reported accuracy of indoor positioning systems (IPSs) is different. For example, UWB and SLAM can achieve centimeter-level precision, while using WiFi or magnetic field generally obtains meter-level accuracy. From the perspective of investment cost, deploying more UWB anchors, WiFi access points (AP), or mechanical equipment in SLAM is expensive, which limits the application of these approaches in large-scale environments. Magnetic positioning, uVLP and PDR need no infrastructure deployment, but the localization accuracy is low. Currently, there is no IPS that can balance the localization accuracy and investment cost [10].

IPSs can use a fingerprinting approach or a ranging-based technique. Fingerprinting-based IPSs need a pre-built database for online matching, like the image database [6], magnetic field map [7], light map [11], or radio map [12]. Matching algorithms including *k*-nearest neighbors (KNN) [7], deep learning [13], etc., have been proposed. Fingerprinting is easier to be implemented on phones and provides considerable precision. However, the measurement (update) campaigns of the fingerprint database are always labour-intensive and complex. Ranging-based IPS can be realized by leveraging UWB [3] or WiFi FTM [14]. Basically, three or more anchors should be deployed in the environments, and the location of the undetermined object is calculated based on trilateration algorithms [3], [14]. There is no lab-intensive measurement work in ranging-based IPS and the positioning precision is usually higher than that of fingerprinting-based IPS. However, the ranging process is impacted by indoor topologies, which bring non-line-of-sight (NLoS) and multipath errors, making the ranging-based IPS inaccurate. Meanwhile, with the development of inertial measurement units (IMUs), the PDR approach has also attracted much attention. PDR needs no fingerprint database or ranging data, and outputs positions consequently based on IMU sensors. However, it is severely affected by pedestrian walking behaviors, and system errors accumulate quickly over time [8], which still need mitigation approaches.

Localization can be performed on mobile phones by using the WiFi/Bluetooth modules, cameras, or embedded IMU sensors. With the new version of the IEEE 802.11mc wireless local area work (WLAN) standard [15], mobile phones can directly communicate with the APs to measure the round-trip-time (RTT) of WiFi signals based on the FTM protocol [16], making smartphone-based WiFi FTM positioning (WFP) popular. In a line-of-sight (LoS) indoor scenario, it has been proved that the WiFi FTM ranging and positioning can obtain considerable accuracy [17]. However, indoor environments often have a lot of non-line-of-sight links, making FTM ranging more complex. Research work in [18] reports that the WiFi FTM positioning does not work well in such scenarios. Therefore, many works have been performed to improve the precision. Methods such as map/FTM fusion [16], WFP/PDR fusion model [19], NLoS/LoS identification [20], temporal-spatial constraints strategy [21], etc., have been presented.

Final version: DOI: 10.1109/IPIN54987.2022.9918110

Among these works, the WiFi ranging data is mainly used for localization, and the WiFi received signal strength (RSS) always plays a supporting role for ranging-based localization, such as NLoS/LoS identification based on the variances of RSS and ranging data [20], or using the RSS-based range to improve the accuracy of WiFi ranging [22]. Since the RSS is simultaneously measured during the WiFi ranging process, it is necessary to study whether the localization using RSS is an effective addition to the WFP in indoor scenarios.

Motivated by this, we carried out experiments to test the FTM fingerprinting using theoretical RSS, ranging data, and proposed a PF-based WiFi FTM fingerprinting approach. Considering the labour-intensive fingerprint collection work, we compare both a distance-based path loss model and a heuristic WHIPP tool [23] to construct the fingerprint database. During online matching, the PF is adopted to reduce mismatching. The map information is introduced to optimize the resampling strategy of the particle filter. The accurate position is estimated after applying the map-aided PF. Our contributions are as summarized follows:

1) We evaluate the WiFi FTM fingerprinting in two environments by using ranging data, theoretical RSS, and mixed theoretical RSS/ranging data, and prove that the mixed fingerprint improves the accuracy and stability of FTM fingerprinting.
2) We propose an accurate WiFi FTM fingerprinting approach based on a map-assisted particle filter. This method can effectively reduce the mismatching of fingerprinting and improve localization accuracy without the labour-intensive fingerprint measurement campaign.
3) We conduct extensive experiments in two different NLoS and mixed LoS/NLoS environments to test the proposed PF-based methods and confirm that it provides generally usable localization results. The poor performance of the ranging-based WiFi positioning is well addressed.

The remainder of this paper is organized as follows: Section II describes the related works on WFP; Section III presents the architecture of the proposed method; Section IV shows the experimental results, and Section V draws the conclusions.

II. Related Works

Since the new version of the IEEE 802.11mc WLAN standard [15] was released in 2016, the distance between the WiFi initiator stations and the responder stations can be estimated based on the FTM protocol. To test the FTM ranging, Banin *et al* [16] first investigated the accuracy of the dynamic WiFi FTM ranging with LIDAR and reported that 90% of the FTM measurements at a distance of 10 m obtained a ranging precision within 1 m. Based on this, they utilized the Bayesian filter solution and map information to perform localization and obtained an accuracy of about 3 m in 90% of the cases. In [18], the "FUSIC" method is designed to address the low-accuracy ranging problem in NLoS conditions. "FUSIC" can extend FTM's LoS accuracy to NLoS settings, providing room-level positioning accuracy. In [24], the key factors that affect the WiFi ranging are studied and the standard error correction technique is proposed. The testing results show that meter-level ranging accuracy is possible in an open outdoor space. In [25], an artificial neural network is adopted to improve the ranging accuracy and obtains a ranging error below 4 m in 90% of the cases, which outperforms the maximum likelihood estimation method. These works validate the WiFi FTM ranging and localization performance, and provide good references for the research on smartphone-based WiFi FTM positioning.

Mobile phones have started to support WiFi FTM since the Android Pie system was released in 2018. Smartphone-based FTM ranging needs no time synchronization like the time of arrival (TOA)-based [26] and time difference of arrival (TDOA)-based [27] WiFi ranging approaches. This revolutionary update makes the smartphone-based WFP popular. Therefore, many types of research have appeared. Yu *et al* [17] first investigated the FTM ranging performance on phones and confirm that meter-level ranging accuracy can be obtained in LoS conditions after error compensation, and the localization precision is within 2.2 m. However, real-life indoor environments lead to serious NLoS/multipath errors on WiFi ranging, making the WFP very inaccurate. Researchers have developed different approaches from different perspectives to solve this problem. Yu *et al* [19] integrate the WFP with PDR based on the unscented particle filter (UPF) to improve the positioning accuracy, and the results show that this UPF-based fusion model can deliver accuracy within 1.15 m. In [28], a least square-based WiFi ranging compensation method is built and an extended Kalman filter-based WFP/PDR fusion model is constructed. Meter-level fusion positioning is reached in a low-NLoS environment. Apart from fusion models, some works process the WiFi ranging data or design optimization strategies to improve accuracy. In [20], the features of the WiFi RSS and ranging data in LoS/NLoS environments are extracted and classified by using a Gaussian model. The testing results reveal that LoS/NLoS identification helps to improve localization performance. Shao *et al* [21] convert the ranging measurements at different places into multiple virtual positioning clients to attenuate the effect of the multipath problem and propose a Karush-Kuhn-Tucker (KKT)-constrained temporal-spatial optimization strategy for position estimation. This method reaches a submeter-level positioning accuracy in 80% of the cases in complex indoor environments. In [22], the WiFi FTM ranging accuracy is improved by fusing the RSS-based range based on the Kalman filter. Experimental results show that the ranging errors are reduced by 31.64% (outdoor) and 23.74% (indoor). The mean localization accuracy is within 1.5 m in a real-life indoor environment.

To summarize, current WiFi FTM positioning researches mainly concentrate on the ranging-based approaches. Although some works adopt RSS for the research, RSS serves as a supporting input variable for WiFi ranging. The collaboration of RSS and ranging data in localization has not been investigated in depth. In this work, we further investigate the fingerprinting performance by using RSS and ranging data, and develop a particle filter-based WiFi FTM fingerprinting approach.

III. METHODS

A. Architecture

Fig. 1 shows that the PF-based WiFi FTM fingerprinting method consists of an offline phase and online phase. There are two different methods for the offline database construction and online matching. We denote these two methods as "Method A" (*Section B.2*) and "Method B" (*Section B.3*).

During the offline phase, Method A first divides the testing area into grid points. Then, an artificial WiFi database is constructed by integrating the theoretical RSS and distance sequences. This work needs to train the path loss (PL) model of the WiFi propagation based on the RSS measurements of ground-truth points. Then, the plane distances between the grid points and access points are calculated. The theoretical RSS is computed based on the PL model and plane distance. The WiFi database is built by combining the theoretical RSS, plane distance, and the corresponding coordinates. Method B utilizes the WHIPP tool [23] to generate the WiFi database with no prior WiFi measurements for PL model training.

During the online phase, Method A first transforms the measured ranging data to the theoretical RSS based on the PL model. Then, the measured RSS and theoretical RSS are integrated using the Kalman filter. The filtered RSS and measured ranging data are used for online KNN matching. Method B first calibrates the measured RSS, and then the calibrated RSS and ranging data are used for online KNN matching. Finally, the map information and the KNN-based locations (derived from Method A or Method B) are input into the PF model for accurate position estimation.

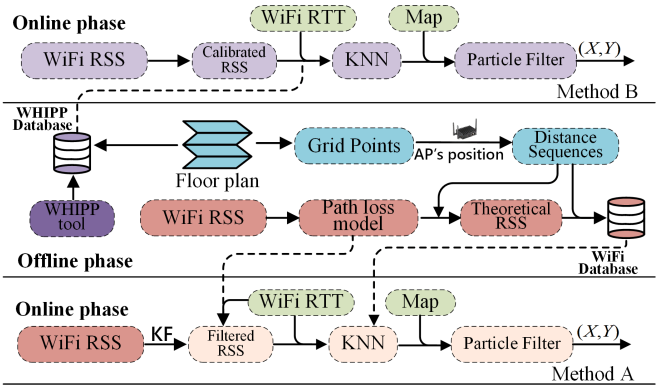

Fig. 1. Flow graph of the proposed method.

B. WiFi FTM ranging and Fingerprinting

1) WiFi FTM Ranging: Fig. 2 shows that the WiFi FTM is the process of measuring the exchanging time of the FTM request and acknowledge (ACK) message. The ranging process starts after the WiFi AP responds to the FTM request. Smartphone and AP capture the corresponding timestamps when the FTM request and ACK message depart or arrive. If there are n successful exchanges, the distance D between the AP and mobile phone is calculated as:

$$D = \frac{C}{2n}\sum_{k=1}^{n}([t_4(k) - t_1(k)] - [t_3(k) - t_2(k)]) \quad (1)$$

where C is the speed of light, $t_1(k)$ and $t_2(k)$ are the time-of-departure (ToD) and time-of-arrival (ToA) of the FTM package, $t_3(k)$ and $t_4(k)$ are the ToD and ToA of the ACK message, respectively. The smartphone can simultaneously measure the distances with respect to multiple APs. However, the WiFi FTM ranging is easily affected by the indoor scenarios, making the ranging-based positioning not efficient.

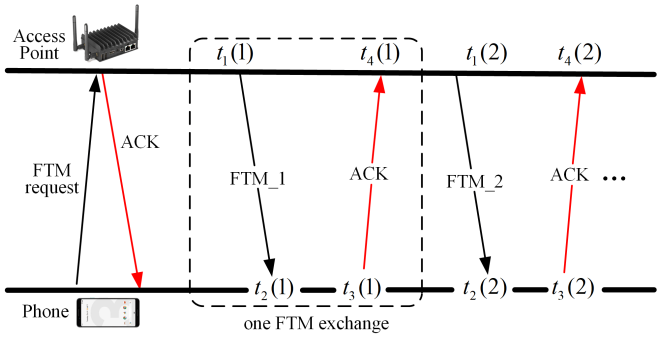

Fig. 2. Description of the FTM producer.

2) Method A-WiFi FTM Fingerprinting with distance-based fingerprint: Instead of a full manual fingerprinting at all the reference points, we build a mixed theoretical RSS/RTT fingerprint database by using a mathematical method. The only offline measurement work is to measure RSS at some ground-truth points and construct a distance-based path loss model [22], which defines the relationship between the theoretical RSS and plane distance as follows:

$$P_i = P_0 - 10\beta\log_{10}(d_i/d_0) + \kappa \quad (2)$$

where P_0 and P_i are the WiFi RSS at the distance d_0 and d_i, d_0 is usually 1 m; β represents the path loss exponent, κ is a random error, respectively. As Fig. 3 shows, the PL models of different APs could be obtained by fitting the measured RSS as a function of ground-truth distances. These PL models are used for constructing a fingerprint database per AP.

Before the WiFi database construction, a division of the positioning area into grid points (GP) should first be made. The plane distance between the GP and the AP is calculated:

$$d_i = \sqrt{(x - \tilde{x}_i)^2 + (y - \tilde{y}_i)^2} \quad (3)$$

where (x, y) and $(\tilde{x}_i, \tilde{y}_i)$ are the coordinates of the GP and the $i-th$ AP, respectively. Based on (2) and (3), the theoretical RSS values at each grid point can be calculated. Then, the fingerprint η_i at the $i-th$ grid point is defined as:

$$\eta_i = [RSS_{i1}, RSS_{i2}, ..., RSS_{im}, d_{i1}, d_{i2}, ..., d_{im}, x_i, y_i] \quad (4)$$

where m is the number of APs, (x_i, y_i) is the position of the $i-th$ grid point, respectively.

During the online positioning phase, the measured ranging data is used to estimate the theoretical RSS based on the PL model. Then, the measured RSS and theoretical RSS are integrated by using the Kalman filter, which is expressed as:

$$\begin{cases} \boldsymbol{S}_k = \boldsymbol{A}\boldsymbol{S}_{k-1} + \boldsymbol{W}_{k-1} \\ \boldsymbol{Z}_k = \boldsymbol{H}\boldsymbol{G}_{k-1} + \boldsymbol{V}_k \end{cases} \quad (5)$$

where $\boldsymbol{S}_k$ and $\boldsymbol{S}_{k-1}$ are the system states (theoretical RSS values) at the time k and $k-1$, $\boldsymbol{A}$ and $\boldsymbol{H}$ are the transition and

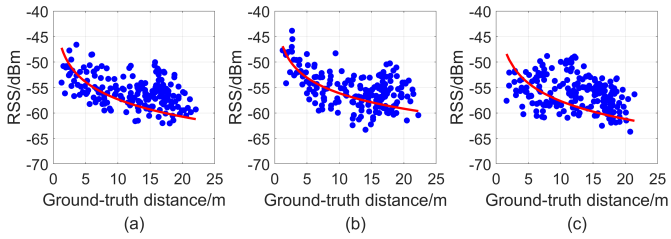

Fig. 3. Fitting curves of path loss models of three APs.

observation matrices, $\boldsymbol{A}=\boldsymbol{I}_{1\times1}$ and $\boldsymbol{H}=\boldsymbol{I}_{1\times1}$; $\boldsymbol{Z}_k$ and $\boldsymbol{G}_{k-1}$ are the systematic observation and the measured RSS; $\boldsymbol{W}_{k-1}$ and $\boldsymbol{V}_k$ are the system and measurement noise, respectively. The complete filter process is executed as:

(a) System state prediction:

$$\boldsymbol{S}_k^- = \boldsymbol{A}\boldsymbol{S}_{k-1} + \boldsymbol{W}_{k-1} \tag{6}$$

(b) System variance matrix prediction:

$$\boldsymbol{P}_{k-1}^- = \boldsymbol{A}\boldsymbol{P}_{k-1}\boldsymbol{A}^T + \boldsymbol{Q}_{k-1} \tag{7}$$

where $\boldsymbol{Q}_{k-1}$ is the variance matrix of the system noise $\boldsymbol{W}_{k-1}$.

(c) System observation estimation using the measured RSS value at the time k:

$$\boldsymbol{Z}_k = \boldsymbol{H}\boldsymbol{G}_k + \boldsymbol{V}_k \tag{8}$$

(d) Calculate the Kalman gain (KG):

$$\boldsymbol{K}_k = \boldsymbol{P}_k^-\boldsymbol{H}^T[\boldsymbol{H}\boldsymbol{P}_{k-1}\boldsymbol{H}^T + \boldsymbol{R}_k] \tag{9}$$

(e) System state updated by the system prediction, KG, and the systematic observation:

$$\boldsymbol{S}_k = \boldsymbol{S}_k^- + \boldsymbol{K}_k[\boldsymbol{Z}_k - \boldsymbol{H}_k\boldsymbol{S}_k^-] \tag{10}$$

(f) System variance matrix update:

$$\boldsymbol{P}_k = (\boldsymbol{I} - \boldsymbol{K}_k\boldsymbol{H})\boldsymbol{P}_k^- \tag{11}$$

For online matching, the measured RSS and the theoretical RSS are integrated by performing (a)∼(f), and the filtered RSS is combined with the measured ranging data using (4). The KNN method [7] is leveraged to assess the similarities against the constructed WiFi database. The estimated position is input into the PF model for accurate tracking.

3) Method B-WiFi FTM Fingerprinting with WHIPP-based fingerprint: Apart from using the prior measurement information to train the PL Model and construct the WiFi database, we also generate the WiFi database based on an automatic WHIPP tool [23]. WHIPP estimates the received power at the different locations in the building, avoiding an expensive and time consuming measurement campaign. Constructing the radio maps only requires drawing the floor plan with the right materials in the tool. The radio map construction builds on an advanced heuristic path loss model that was constructed and validated based on measurements in different building types (office, congress center, arts center). The PL model is as:

$$PL_i = PL_0 + 10\beta\log_{10}(d_i) + \sum L_W + \sum L_I \tag{12}$$

where PL_i is the total path loss along a path distance d_i, P_0 is the path loss at a distance of d_0, $\sum L_W$ is the total wall loss along the path, $\sum L_I$ is the accumulated interaction loss along the path, β denotes the path loss exponent, respectively. Moreover, before online matching, the measured RSS should be first calibrated:

$$r_{ij}^m = ar_{ij}^w + b \tag{13}$$

where r_{ij}^m and r_{ij}^w represent the measured and the WHIPP-based RSS values at location i from the $j-th$ AP, a and b are the parameters for mapping the RSS values from WHIPP to the measured data. The details for calibration can be found in [29]. In this method, there is no need to train a PL model. The calibrated RSS and measured ranging data are input into the KNN algorithm to perform online matching against the WHIPP-based database.

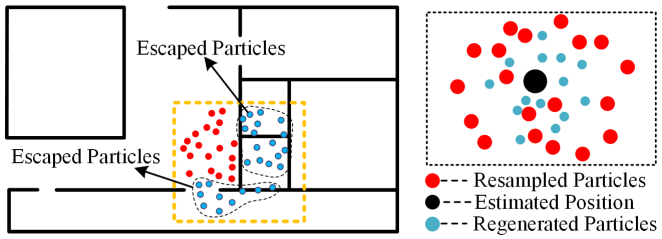

Fig. 4. Resampled particles with map constraint.

C. Fingerprinting with Map-assisted Particle Filter

PF is a good technique for dealing with the optimal estimation of a nonlinear system by combining the known states, modeling assumptions, and observations information. More details about the particle filter model are given in [14]. In this work, we summarize the proposed WiFi FTM fingerprinting with map-assisted PF as follows:

Step 1: *Initialization*. Performing PF needs a particle swarm with N particles. The first step is to generate particles that are uniformly distributed over the testing area. Every particle has attributes that are the same with the format of fingerprint, which is expressed as:

$$\Xi = [rss_{j1}, ..., rss_{ji}, ..., rss_{jm}, d_{j1}, ..., d_{ji}, ..., d_{jm}, \omega_j, \hat{x}_j, \hat{y}_j] \tag{14}$$

where m is the number of APs, $(\hat{x}_j, \hat{y}_j)$ and ω_j represent the position and the initial weight of the $j-th$ particle, $j = 1, ..., N$; rss_{ji} and d_{ji} are obtained by assigning random values in a range 0∼2 to the measured RSS and ranging data, $i = 1, ..., m$, respectively. The initial value of ω_j is $\frac{1}{N}$. The map information is simultaneously loaded in this step.

Step 2: *Update and normalize the weights of particles*. For the filtering at the timestamp k, the KNN-based fingerprinting gives an estimated position as the system state of the PF. Based on this, all the particles' weights are updated as:

$$\omega_j = \frac{1}{\sqrt{2\pi\sigma}} exp(-\frac{h_j^2}{2\sigma^2}) \tag{15}$$

where σ is the system variance, h_j is calculated as:

$$h_j = \sum_{i=1}^{n}(|rss_{ji} - R_{ki}| + |d_{ji} - l_{ki}| + |\overline{x}_k - \hat{x}_j| + |\overline{y}_k - \hat{y}_j|) \tag{16}$$

where $(\hat{x}_j, \hat{y}_j)$, rss_{ji} and d_{ji} are the same as the variables in (14), l_{ki} and R_{ki} represent the measured distance and the filtered RSS from the $i-th$ AP at the time k, $(\overline{x}_k, \overline{y}_k)$

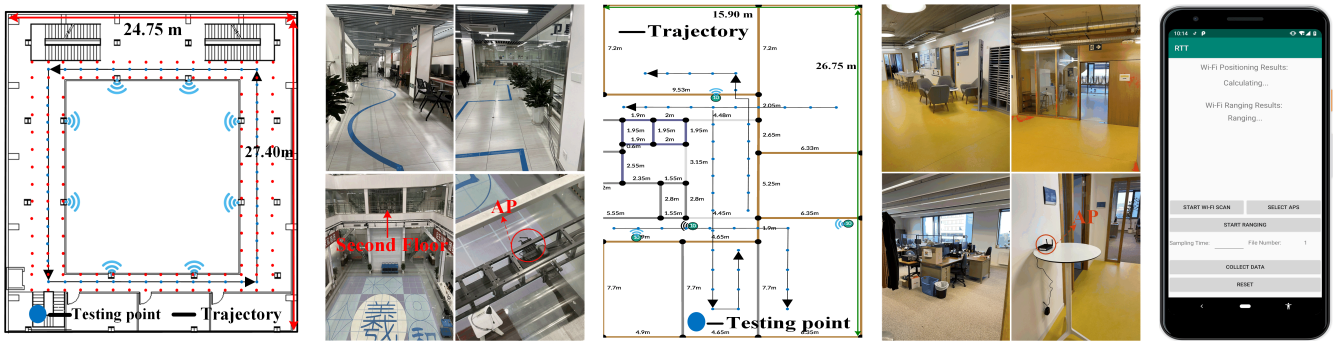

(a) (b) (c) (d) (e)

Fig. 5. Experimental setup. (a) Floor plan of SKSET, (b) Office scenarios of SKSET, (c) Floor plan of iGent 5-th floor, (d) Office scenarios of iGent 5-th floor, (e) Pixel 3 phone and developed data acquisition software.

are the coordinates of the KNN-based position. Then, the normalization of particles' weights is performed by:

$$\omega_j^{'} = \frac{\omega_j}{\sum_{j=1}^{N} \omega_j} \tag{17}$$

where $\omega_j^{'}$ is the normalized weight of the $j-th$ particle.

Step 3: *Resampling with map constraint*. This step is to select the particles with larger weights based on the normalized weights. In this work, we apply a multinomial resampling method [30]. For the resampled particle swarm, the map information is adopted to remove the "escaped" particles. As Fig. 4 shows, the map information (walls, corridors, etc.) is extracted based on the KNN-based position. The geometric relationships between the extracted map information and the resampled particles are evaluated. We define the particles that cross the walls or enter inaccessible areas as "escaped", and remove them from the swarm. If there are no "escaped" particles, the resampled swarm remains to the next step.

Step 4: *Calculate the filtered result*. The weighted coordinates of the remained resampled particles are output as the filtered results. The definition is as follows:

$$\begin{cases} X = \frac{1}{m} \sum_{j=1}^{m} \omega_j^{'} \hat{x}_j \\ Y = \frac{1}{m} \sum_{j=1}^{m} \omega_j^{'} \hat{y}_j \end{cases} \tag{18}$$

where (X, Y) represents the final estimated position, m is the number of the remaining particles in the swarm, $m \leq N$. To keep the size of the particle swarm, $(N-m)$ particles will be regenerated around the final estimated position with a uniform distribution and added to the particle set.

IV. Experiments

A. Experimental Setup

We test the proposed approaches in the state key laboratory of satellite navigation system and equipment technology (SKSET, Shijiazhuang, China) and the 5-th floor of the iGent building (Ghent, Belgium).

The SKSET is a typical real-life office scenario. 8 WiFi RTT APs with the hardware part of Intel Dual Band Wireless-AC8260 are installed outside the corridors of the second floor (Fig. 5(a) and 5(b)). The concrete and glass walls make the NLoS condition for WiFi measurement. During the offline stage, we first use Method A to generate a PL model-based database (PLMD). The PL models are trained with the WiFi measurements on 172 modeling points. After that, this testing area is divided into 1756 grid points (GPs) with a separation of 0.3 m. The theoretical RSS values and plane distances of every GP with respect to APs are calculated by using (2) and (3), respectively. The PLMD database is constructed by combining the theoretical RSS, plane distance, and the corresponding coordinates. Method B generates a WHIPP-based database with 4162 GPs. Testing data are collected three times on 64 testing points by using a Pixel 3 phone (Fig. 5(e)) with a sampling rate of 5 Hz.

The 5-th floor of the iGent building is a typical office environment (Fig. 5(c) and 5(d)), where are installed 3 WiFi RTT APs (same as the APs in SKSET) and one commercial AP. These APs make a mixed NLoS/LoS condition. For the PLMD database construction, the PL models are trained with 50 modeling points. The testing area is divided into 4717 GPs with a separation of 0.3 m. The PLMD database is built by using Method A. Method B generates a WHIPP-based database with 9361 GPs. Testing data is collected three times on 50 testing points by using a Pixel 3 phone with a sampling rate of 2 Hz.

The positioning tests contain static fingerprinting tests (referred to the testing points in Fig. 5(a) and 5(c)) and dynamic PF simulation (referred to the trajectories in Fig. 5(a) and 5(c)). All the data analyses of these two experiments are made on a laptop with 8 GB RAM and a 2.6 GHz CPU.

TABLE I
Fingerprinting Approaches and Descriptions

Database	Subsets	Online matching description
PLMD (Method A)	TRSS	Filtered theoretical RSS using (6)-(11)
	RTT	Measured ranging data
	TRSS/RTT	Mixed TRSS/RTT fingerprint
WHIPP (Method B)	WRSS	Calibrated RSS using (13)
	WRTT	Measured ranging data
	WRSS/WRTT	Mixed WRSS/WRTT fingerprint

B. Static fingerprinting tests in SKSET and iGent

Table I shows the fingerprinting methods using different data and online matching details. Table II and Fig. 6 show the static fingerprinting results in the two different testing sites.

TABLE II
ERRORS COMPARISON OF FINGERPRINTING BASED ON DIFFERENT DATABASES

Database	Subsets	SKSET					iGent				
		Min/m	Max/m	Mean/m	RMSE/m	75%Error/m	Min/m	Max/m	Mean/m	RMSE/m	75%Error/m
PLMD	TRSS	0.33	9.45	2.92	3.36	3.92	0.16	11.27	2.82	3.75	3.46
	RTT	0.22	9.42	2.59	3.05	3.63	0.18	13.79	2.52	3.81	2.80
	TRSS/RTT	0.15	7.92	2.23	2.70	3.22	0.12	13.11	2.38	3.58	2.49
WHIPP	WRSS	0.13	9.92	3.14	3.76	4.57	0.27	11.89	2.95	3.77	3.84
	WRTT	0.14	9.72	2.73	3.24	3.88	0.26	14.08	2.62	3.89	2.72
	WRSS/WRTT	0.13	9.53	2.53	3.07	3.68	0.36	9.30	2.51	3.30	2.92

When using the PLMD database, directly performing TRSS fingerprinting in SKSET (NLoS condition) only delivers a mean positioning error (ME) of 2.92 m, and the root-mean-square error (RMSE) is 3.36 m. The ME and RMSE of the RTT fingerprinting are 2.59 m and 3.05 m, which are better than those of the TRSS fingerprinting. However, based on the mixed TRSS/RTT fingerprint, the localization accuracy is improved to 2.23 m, and the RMSE decreases to 2.70 m. Compared to the TRSS method, the ME and RMSE of the TRSS/RTT are reduced by 21.23% and 19.64%, respectively. Similarly, compared to the RTT fingerprinting, the ME and RMSE of the proposed method are reduced by 13.90% and 11.47%, respectively. For the fingerprinting against the WHIPP database in SKSET, the mixed WRSS/WRTT obtains a ME of 2.53 m, and the RMSE is 3.07 m. The ME and RMSE are reduced by 19.4% and 18.35% compared to the WRSS fingerprinting, respectively. These results demonstrate that WiFi FTM fingerprinting using the mixed ranging data and theoretical RSS improve the mean positioning accuracy.

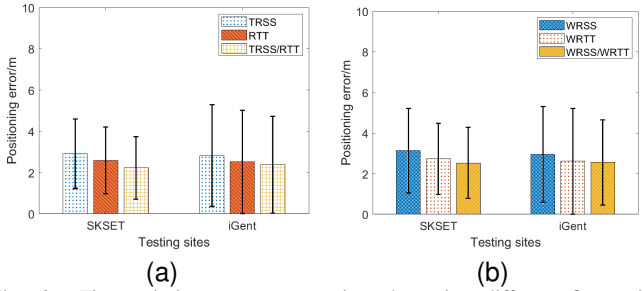

Fig. 6. Fingerprinting errors comparison by using different fingerprint databases in different testing sites. (a) PLMD database; (b) WHIPP database

For the testing results using WHIPP Database in iGent (mixed NLoS/LoS condition), the ME of the WRSS-based positioning is 2.95 m, which is improved to 2.51 m by using the mixed WRSS/RTT fingerprint. Although the mixed fingerprint improves the localization accuracy, it is not improved much compared to the WRTT-based fingerprinting. This is because of the instability of WRTT-based fingerprinting, which has the largest RMSE of 3.89 m. Regarding the results using PLMD database, mixed TRSS/RTT improves positioning accuracy, delivering a ME of 2.38 m and an RMSE of 3.58 m. The RTT fingerprinting is still unstable with an RMSE of 3.81 m. Fig. 6 shows the fluctuations of RTT-based and WRTT-based fingerprinting in iGent, where the limited RTT APs cause the unstable positioning. However, Fig. 6 and Table II show that the stability and localization accuracy are better improved when using mixed RSS and ranging data for fingerprinting in these two testing sites. We conclude that using the mixed fingerprint improves localization performance of WiFi FTM fingerprinting in both NLoS and mixed NLoS/LoS conditions.

TABLE III
PF-BASED APPROACHES AND DESCRIPTIONS

Approaches	Description	Fingerprinting
TRSS-PF	PF tracking based on TRSS	Method A
RTT-PF	PF tracking based on RTT	Method A
WRSS-PF	PF tracking based on WRSS	Method B
WRTT-PF	PF tracking based on WRTT	Method B
Proposed	PF tracking using TRSS/RTT	Method A
	PF tracking using WRSS/WRTT	Method B

C. Dynamic PF tracking simulation in SKSET and iGent

We compare the proposed methods with the WiFi ranging-based approaches of using weighted least square (WLS) [28], RSS/FTM range fusion [22]. Combining the fingerprinting descriptions in Table I, the details of PF-based methods are shown in Table III. The numbers of the particles of all the PF-based approaches are set as 1000. Table IV and Fig. 7 show the testing results.

Table IV shows that performing classic WLS in SKSET only obtains a ME of 3.77 m and an RMSE of 4.37 m. The RSS-FTM improves accuracy, while the ME and RMSE are only reduced by 0.52 m and 0.63 m, respectively. Compared to the PF-based fingerprinting methods, the positioning accuracy of these two ranging-based methods is worse. TRSS-PF and RTT-PF can deliver a ME within 2.13 m, the RMSE of TRSS-PF is slightly lower than that of the RTT-PF approach. The ME and RMSE of the proposed method are 1.70 m and 2.17 m, which are the best results of these methods. Compared to WLS, the ME and RMSE are reduced by 54.91% and 50.34%, respectively. When using the WHIPP database, the proposed method delivers an accuracy and RMSE of 2.07 m and 2.61 m, which are improved by 45.09% and 40.27% compared to WLS, respectively. For a confidence level of 75%, the proposed methods obtain the best accuracy. Fig. 7(a) and 7(b) show that PF tracking using TRSS/RTT or WRSS/RTT can deliver the best results compared to other methods. These experimental results prove that the proposed approach performs well in an NLoS scenario and outperforms the classic ranging-based methods.

TABLE IV
ERRORS COMPARISON OF WIFI POSITIONING METHODS

Database	Methods	SKSET					iGent				
		Min/m	Max/m	Mean/m	RMSE/m	75%Error/m	Min/m	Max/m	Mean/m	RMSE/m	75%Error/m
/	WLS	0.37	11.20	3.77	4.37	5.08	0.23	22.70	3.39	4.15	3.66
	RSS-FTM	0.32	11.35	3.25	3.74	4.17	0.18	22.21	3.25	3.78	3.97
PLMD	TRSS-PF	0.16	6.45	2.11	2.60	3.11	0.09	17.53	2.30	3.26	1.99
	RTT-PF	0.14	8.14	2.13	2.70	3.23	0.07	15.34	2.11	3.15	1.67
	Proposed	0.04	6.40	1.70	2.17	2.31	0.05	11.97	1.85	2.55	1.50
WHIPP	WRSS-PF	0.08	8.76	2.24	2.98	3.14	0.06	11.43	2.37	2.54	2.69
	WRTT-PF	0.05	6.84	2.16	2.72	3.34	0.02	13.67	2.03	2.79	1.75
	Proposed	0.05	7.76	2.07	2.61	2.96	0.08	14.30	1.92	2.38	1.69

For the testing results in iGent, directly performing WLS obtains a ME of 3.39 m, and the RMSE is 4.15 m. The maximal positioning error of WLS is 22.70 m, which indicates the instability of WLS. Using the RSS-FTM approach improves accuracy, with only an improvement of 0.14 m. The PF-based fingerprinting methods still perform better than the ranging-based methods. By using the mixed WRSS/WRTT fingerprint, the ME and RMSE are 1.92 m and 2.38 m, which are the best results of the PF-based approaches using WHIPP-based database. Compared to the WLS, the ME and RMSE are decreased by 43.36% and 42.65%, respectively. The instability of WRTT-based fingerprinting also leads to the unstable WRTT-PF, which has the largest RMSE (2.79 m). On the other hand, when using the PLMD database, PF tracking based on TRSS/RTT obtains an accuracy and RMSE of 1.85 m and 2.55 m, which are improved by 45.43% and 38.55% compared to WLS, respectively. Fig. 7(c) and 7(d) demonstrates that the PF-based fingerprinting methods outperform the classic ranging-based WiFi FTM positioning under different confidence levels in iGent.

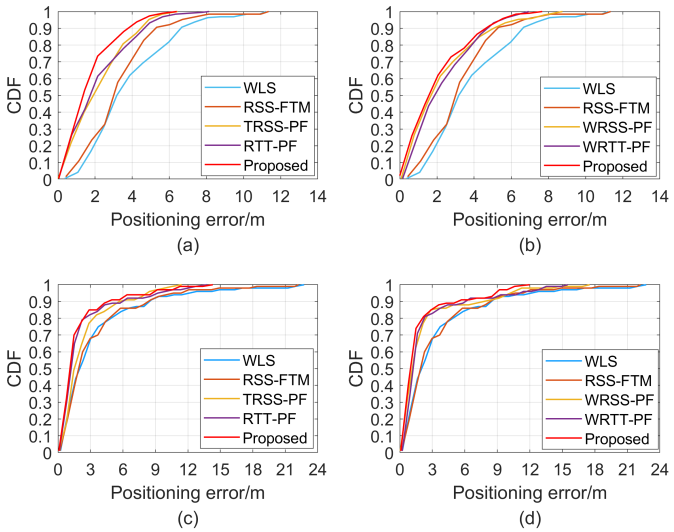

Fig. 7. Cumulative distribution functions comparison of different WiFi positioning methods. (a) Use PLMD database in SKSET; (b) Use WHIPP database in SKSET; (c) Use WHIPP database in iGent; (b) Use PLMD database in iGent.

Combining the results of the two environments, we conclude that the PF-based WiFi FTM fingerprinting works well in NLoS and mixed NLoS/LoS conditions. A complete manual WiFi database generated by the WHIPP tool serves well for the proposed method. As a fingerprinting method, it needs no manual measurement campaign, making up for the labour-intensive shortcoming of the traditional fingerprinting approach.

D. Discussion

For the localization in real-life environments, the proposed FTM fingerprinting based on the map-aided particle filter obtains MEs of 1.70 m and 2.07 m in an NLoS condition and MEs of 1.85 m and 1.92 m in a mixed NLoS/LoS condition, which outperforms the range-based approaches of using WLS [28] and RSS/FTM range fusion [22]. As a fingerprinting approach, it does not suffer from the NLoS or multipath problems, which make the WiFi ranging accurate. The NLoS/LoS identification [20] improves the accuracy of WiFi ranging positioning, and the reported accuracy improvement is about 36.4%. However, the accuracy of our method is improved by at most 54.91% and 45.43% in the NLoS and mixed NLoS/LoS conditions, respectively. On the other hand, training NLoS/LoS identification model [20] and ANN ranging model [25] need a large amount of WiFi data, our method needs no measurement campaign and can be deployed based on the WHIPP tool. Compared to the ranging-based method using the complex temporal-spatial constraints [21], fingerprinting is easier to implement and the localization accuracy is satisfactory with the map-aided particle filter. Moreover, the testing results prove that the combination of RSS and ranging data improves the FTM fingerprinting accuracy. The efficiency of the PF-based FTM fingerprinting provides an effective approach for the localization using WiFi in real-life scenarios.

V. CONCLUSION

In this work, a novel WiFi FTM fingerprinting using a map-aided particle filter is proposed to address the poor performance of the range-based WFP. The experimental results in two different testing sites prove that using the mixed Theoretical RSS/RTT improves the accuracy of FTM fingerprinting, and demonstrate the PF-based WiFi FTM fingerprinting approach delivers a mean accuracy of within 2 m in NLoS and mixed NLoS/LoS conditions. In the future, we will study more

accurate fingerprinting methods by integrating RTT APs and more commercial APs, and adopt smartphone IMU sensors to obtain stable and accurate indoor localization.

REFERENCES

[1] Y. Li, Y. Zhuang, P. Zhang, H. Lan, X. Niu, and N. El-Sheimy, "An improved inertial/wifi/magnetic fusion structure for indoor navigation," *Information Fusion*, vol. 34, pp. 101–119, 2017.

[2] G. De Blasio, A. Quesada-Arencibia, C. R. García, J. C. Rodríguez-Rodríguez, and R. Moreno-Díaz, "A protocol-channel-based indoor positioning performance study for bluetooth low energy," *IEEE Access*, vol. 6, pp. 33 440–33 450, 2018.

[3] G. De Angelis, A. Moschitta, and P. Carbone, "Positioning techniques in indoor environments based on stochastic modeling of uwb round-trip-time measurements," *IEEE Trans. Intell. Transp. Syst.*, vol. 17, no. 8, pp. 2272–2281, 2016.

[4] C. Li, E. Tanghe, D. Plets, P. Suanet, J. Hoebeke, E. De Poorter, and W. Joseph, "Reloc: Hybrid rssi-and phase-based relative uhf-rfid tag localization with cots devices," *IEEE Trans. Instrum. Meas.*, vol. 69, no. 10, pp. 8613–8627, 2020.

[5] Y. Chen, R. Chen, M. Liu, A. Xiao, D. Wu, and S. Zhao, "Indoor visual positioning aided by cnn-based image retrieval: training-free, 3d modeling-free," *Sensors*, vol. 18, no. 8, p. 2692, 2018.

[6] T. Taketomi, H. Uchiyama, and S. Ikeda, "Visual slam algorithms: A survey from 2010 to 2016," *IPSJ Trans. Comput. Vis. Appl.*, vol. 9, no. 1, pp. 1–11, 2017.

[7] M. Sun, Y. Wang, S. Xu, H. Cao, and M. Si, "Indoor positioning integrating pdr/geomagnetic positioning based on the genetic-particle filter," *Applied Sciences*, vol. 10, no. 2, p. 668, 2020.

[8] Q. Wang, H. Luo, H. Xiong, A. Men, F. Zhao, M. Xia, and C. Ou, "Pedestrian dead reckoning based on walking pattern recognition and online magnetic fingerprint trajectory calibration," *IEEE Internet Things J.*, vol. 8, no. 3, pp. 2011–2026, 2020.

[9] S. Bastiaens, K. Deprez, L. Martens, W. Joseph, and D. Plets, "A comprehensive study on light signals of opportunity for subdecimetre unmodulated visible light positioning," *Sensors*, vol. 20, no. 19, p. 5596, 2020.

[10] N. El-Sheimy and Y. Li, "Indoor navigation: State of the art and future trends," *Satellite Navigation*, vol. 2, no. 1, pp. 1–23, 2021.

[11] D. Plets, A. Eryildirim, S. Bastiaens, N. Stevens, L. Martens, and W. Joseph, "A performance comparison of different cost functions for rss-based visible light positioning under the presence of reflections," in *Proceedings of the 4th ACM Workshop on Visible Light Communication Systems*, 2017, pp. 37–41.

[12] Y. Tao and L. Zhao, "Fingerprint localization with adaptive area search," *IEEE Commun. Lett.*, vol. 24, no. 7, pp. 1446–1450, 2020.

[13] B. Bhattarai, R. K. Yadav, H.-S. Gang, and J.-Y. Pyun, "Geomagnetic field based indoor landmark classification using deep learning," *IEEE Access*, vol. 7, pp. 33 943–33 956, 2019.

[14] S. Xu, R. Chen, Y. Yu, G. Guo, and L. Huang, "Locating smartphones indoors using built-in sensors and wi-fi ranging with an enhanced particle filter," *IEEE Access*, vol. 7, pp. 95 140–95 153, 2019.

[15] IEEE, "Ieee standard for information technology-telecommunications and information exchange between systems–local and metropolitan area networks-specific requirements–part 11: Wireless lan medium access control (mac) and physical layer (phy) specifications amendment 2: Sub 1 ghz license exempt operation," 2017.

[16] L. Banin, U. Schatzberg, and Y. Amizur, "Wifi ftm and map information fusion for accurate positioning," in *Proc. of the 2016 IPIN*, 2016.

[17] Y. Yu, R. Chen, Z. Liu, G. Guo, F. Ye, and L. Chen, "Wi-fi fine time measurement: Data analysis and processing for indoor localisation," *J. Navig.*, vol. 73, no. 5, pp. 1106–1128, 2020.

[18] K. Jiokeng, G. Jakllari, A. Tchana, and A.-L. Beylot, "When ftm discovered music: Accurate wifi-based ranging in the presence of multipath," in *Proc. of the IEEE INFOCOM 2020*. IEEE, 2020, pp. 1857–1866.

[19] Y. Yu, R. Chen, L. Chen, S. Xu, W. Li, Y. Wu, and H. Zhou, "Precise 3-d indoor localization based on wi-fi ftm and built-in sensors," *IEEE Internet Things J.*, vol. 7, no. 12, pp. 11 753–11 765, 2020.

[20] M. Si, Y. Wang, S. Xu, M. Sun, and H. Cao, "A wi-fi ftm-based indoor positioning method with los/nlos identification," *Applied Sciences*, vol. 10, no. 3, p. 956, 2020.

[21] W. Shao, H. Luo, F. Zhao, H. Tian, S. Yan, and A. Crivello, "Accurate indoor positioning using temporal–spatial constraints based on wi-fi fine time measurements," *IEEE Internet Things J.*, vol. 7, no. 11, pp. 11 006–11 019, 2020.

[22] G. Guo, R. Chen, F. Ye, X. Peng, Z. Liu, and Y. Pan, "Indoor smartphone localization: A hybrid wifi rtt-rss ranging approach," *IEEE Access*, vol. 7, pp. 176 767–176 781, 2019.

[23] D. Plets, W. Joseph, K. Vanhecke, E. Tanghe, and L. Martens, "Coverage prediction and optimization algorithms for indoor environments," *EURASIP. J. Wirel. Commun. Netw.*, vol. 2012, no. 1, pp. 1–23, 2012.

[24] M. Ibrahim, H. Liu, M. Jawahar, V. Nguyen, M. Gruteser, R. Howard, B. Yu, and F. Bai, "Verification: Accuracy evaluation of wifi fine time measurements on an open platform," in *Proc. of the 24th annu. Int. Conf. Mob. Comput. Netw.*, 2018, pp. 417–427.

[25] N. Dvorecki, O. Bar-Shalom, L. Banin, and Y. Amizur, "A machine learning approach for wi-fi rtt ranging," in *Proc. of the 2019 International Technical Meeting of The Institute of Navigation*, 2019, pp. 435–444.

[26] S. A. Golden and S. S. Bateman, "Sensor measurements for wi-fi location with emphasis on time-of-arrival ranging," *IEEE Trans. Mob. Comput.*, vol. 6, no. 10, pp. 1185–1198, 2007.

[27] J. Zhou, L. Shen, and Z. Sun, "A new method of d-tdoa time measurement based on rtt," in *MATEC Web of Conferences*, vol. 207. EDP Sciences, 2018, p. 03018.

[28] M. Sun, Y. Wang, S. Xu, H. Qi, and X. Hu, "Indoor positioning tightly coupled wi-fi ftm ranging and pdr based on the extended kalman filter for smartphones," *IEEE Access*, vol. 8, pp. 49 671–49 684, 2020.

[29] C. Laoudias, R. Piché, and C. G. Panayiotou, "Device self-calibration in location systems using signal strength histograms," *Journal of Location Based Services*, vol. 7, no. 3, pp. 165–181, 2013.

[30] B. Turgut and R. P. Martin, "Restarting particle filters: an approach to improve the performance of dynamic indoor localization," in *Proc. of the 2009 IEEE Global Telecommunications Conference*. IEEE, 2009, pp. 1–7.